BI-TP 2008/02
NSF-KITP-08-39

Sterile neutrino dark matter as a consequence of νMSM-induced lepton asymmetry

Mikko Laine[a,b] and Mikhail Shaposhnikov[c]

[a] *Faculty of Physics, University of Bielefeld, D-33501 Bielefeld, Germany*

[b] *Department of Physics, University of Oulu, FI-90014 Oulu, Finland*

[c] *Institut de Théorie des Phénomènes Physiques, EPFL, CH-1015 Lausanne, Switzerland*

Abstract

It has been pointed out in ref. [1] that in the νMSM (Standard Model extended by three right-handed neutrinos with masses smaller than the electroweak scale), there is a corner in the parameter space where CP-violating resonant oscillations among the two heaviest right-handed neutrinos continue to operate below the freeze-out temperature of sphaleron transitions, leading to a lepton asymmetry which is considerably larger than the baryon asymmetry. Consequently, the lightest right-handed ("sterile") neutrinos, which may serve as dark matter, are generated through an efficient resonant mechanism proposed by Shi and Fuller [2]. We re-compute the dark matter relic density and non-equilibrium momentum distribution function in this situation with quantum field theoretic methods and, confronting the results with existing astrophysical data, derive bounds on the properties of the lightest right-handed neutrinos. Our spectra can be used as an input for structure formation simulations in warm dark matter cosmologies, for a Lyman-α analysis of the dark matter distribution on small scales, and for studying the properties of haloes of dwarf spheroidal galaxies.

June 2008

1. Introduction

Ever since the experimental discovery of neutrino mass differences, there has been a compelling case for the existence of right-handed neutrinos in nature. It turns out, however, to be difficult to determine the parameters associated with them with any precision. Indeed, given that right-handed neutrinos are gauge singlets, their Lagrangian contains explicit (Majorana) mass terms in addition to the usual Yukawa interactions. The known mass differences only constrain certain combinations of the Yukawa couplings and Majorana masses, so that the absolute scale of the Majorana masses cannot be fixed from the existing data.

Recently, it has been pointed out [3, 4] that if the Majorana masses are chosen to be significantly smaller than has been the common choice (this corner of the parameter space was named νMSM, for "neutrino Minimal Standard Model"), then it appears possible to find an amazingly complete description of the main cosmological mysteries that cannot be explained within the Standard Model. Suppose that there are three generations of the right-handed neutrinos, like there are of all other fermions in the Standard Model. Then the lightest right-handed, or "sterile" neutrinos, with masses in the keV range, might serve as (warm) dark matter [5, 2], [6]–[14][1]; the two heavier right-handed neutrinos, with masses in the GeV range and almost degenerate with each other, could account simultaneously for baryogenesis and the observed active neutrino mass matrix [16, 4]; while a non-minimal coupling of the Higgs field in this theory to the Ricci scalar might explain inflation [17]. In fact it can be argued that the νMSM could be a good effective field theory all the way up to the Planck scale [18] (for a similar argument in a related theory, see ref. [19]).

On the quantitative level, though, it is non-trivial to realize all of these possibilities within the νMSM. Consider the explanation of dark matter by the lightest sterile neutrinos, for instance. There are strong experimental constraints from two sides: from the non-observation of an X-ray signal generated by the decay of the dark matter neutrinos on one hand ([20]–[31] and references therein), and from structure formation simulations on the other [32]–[36]. Combining these experimental constraints with the results of theoretical computations of thermal dark matter production due to active-sterile mixing (the so-called Dodelson-Widrow mechanism) [5, 6, 7, 9, 10, 12] appears in fact to all but exclude the warm dark matter scenario [34]–[36], [30][2].

Such a negative conclusion is premature, however. First of all, the structure formation simulations of refs. [34]–[36] assumed the spectrum of the dark matter sterile neutrinos to be *thermal*, with possibly a modest shift of the average momentum towards the infrared, while in reality the deviations from the Fermi-Dirac distribution are substantial [10, 12]. Second, and even more importantly, it has been pointed out in ref. [1] that in the framework of the νMSM

[1] Various cosmological and astrophysical phenomena related to the dark matter sterile neutrinos have been discussed in refs. [15].

[2] Extending the νMSM by an extra scalar field allows for an additional mechanism for dark matter sterile neutrino creation which evades these limits [37, 38, 39]; another relaxation follows if the reheating temperature after inflation is low (in the MeV range) [40, 41, 42].

it is possible to generate a large leptonic chemical potential surviving down to temperatures of a few hundred MeV. In this situation the results of the theoretical computation change dramatically [2, 7], and it becomes easier to explain dark matter with sterile neutrinos.

The purpose of the present paper is to elaborate on the latter possibility. More precisely, we re-compute the dark matter relic density in this situation with the quantum field theoretic methods introduced in refs. [11, 12]; analyse uncertainties related to unknown parameters and poorly known QCD phenomena; and compare with previous computations in the literature. Our main finding is that if lepton asymmetries in the range $n_{\nu_e}/s \gtrsim 0.8 \times 10^{-5}$ exist, where n_{ν_e} refers to the asymmetry in electron-like neutrinos and s is the total entropy density, then the νMSM can indeed account for the observed dark matter abundance. This bound can be consolidated once structure formation simulations have been repeated with the non-equilibrium momentum distributions functions ("spectra") of the sterile neutrinos that we derive. In any case, asymmetries in the range $n_{\nu_e}/s \gtrsim 0.8 \times 10^{-5}$ may be reachable in the so-called **Scenario IIa** of parameter values of ref. [1]. Note that the largest possible asymmetry leading to successful Big Bang Nucleosynthesis corresponds to a chemical potential $|\mu_L/T| \lesssim 0.07$ at $T \sim 1$ MeV (95% CL) [43, 44], meaning $n_{\nu_e}/s \lesssim 2.5 \times 10^{-3}$ in our units (cf. appendix A). The maximal asymmetry which can be produced within the νMSM is somewhat smaller, $n_{\nu_e}/s \lesssim 0.7 \times 10^{-3}$ [1].

It is appropriate to stress that even though our considerations are naturally viewed as a sequel to the lepton asymmetry generated *à la* ref. [1], from a practical point of view the origin of the lepton asymmetry plays no role in the present analysis, nor do the parameters related to the two heaviest right-handed neutrinos. Indeed the only ingredient entering our computation is the absolute value of the lepton asymmetry which, as mentioned, we parametrize through the ratio n_{ν_e}/s. Recalling that the observed baryon asymmetry is $n_B/s \simeq (0.9 - 1.0) \times 10^{-10}$ [45, 46], we hence need to assume a boost of some five orders of magnitude in the leptonic sector. Besides νMSM, another possible origin for such an asymmetry could be the Affleck-Dine mechanism [47], if it takes place below the electroweak scale and is based on a condensate producing many more leptons than quarks.

Our presentation is organized as follows. In Sec. 2 we generalize the formalism of refs. [11, 12] to the charge-asymmetric situation. The resulting equation for the sterile neutrino abundance is integrated numerically in Sec. 3, and the equation for the sterile neutrino spectrum in Sec. 4. We discuss the astrophysical consequences of these results in Sec. 5, and conclude in Sec. 6. In appendix A we recall the relations of our characterization of the lepton asymmetry, through n_{ν_e}/s, to a number of other conventions appearing in the literature. A reader only interested in the phenomenological consequences of our analysis could start directly from Sec. 5.

2. Basic formalism

Our starting point is the Lagrangian

$$\mathcal{L} = \frac{1}{2}\,\bar{\tilde{N}}_1 i\partial\!\!\!/\,\tilde{N}_1 - \frac{1}{2}\,M_1\bar{\tilde{N}}_1\tilde{N}_1 - F_{\alpha 1}\bar{L}_\alpha\tilde{\phi}\,a_R\tilde{N}_1 - F^*_{\alpha 1}\bar{\tilde{N}}_1\tilde{\phi}^\dagger a_L L_\alpha + \mathcal{L}_{\rm MSM}\,, \qquad (2.1)$$

where $\tilde{N}_1$ are Majorana spinors, and the subscript "1" refers to the lightest right-handed neutrino; repeated indices are summed over; M_1 is the Majorana mass that we have chosen to be real in this basis; L_α are the active lepton doublets; $F_{\alpha 1}$ are elements of a complex Yukawa matrix; $\tilde{\phi} = i\tau_2\phi^*$ is the conjugate Higgs doublet; and $a_L \equiv (1-\gamma_5)/2$, $a_R \equiv (1+\gamma_5)/2$ are chiral projectors.

To compute the abundance of N_1 from first principles, we make a number of basic assumptions, following refs. [11, 12]. First of all, we restrict to temperatures below a few GeV, implying that the electroweak symmetry is broken: $\langle\tilde{\phi}\rangle \simeq (v/\sqrt{2}, 0)$, where $v \simeq 246$ GeV is the Higgs field vacuum expectation value. Second, we assume that the mixing angles $\theta^2_{\alpha 1} \equiv |M_D|^2_{\alpha 1}/M_1^2$, where $|M_D|_{\alpha 1} \equiv |vF_{\alpha 1}|/\sqrt{2}$, are very small, $\theta_{\alpha 1} \lesssim 10^{-3}$. Then it is sufficient to restrict to the leading non-trivial order in a Taylor series in $\theta^2_{\alpha 1}$.

The third assumption concerns the flavour structure of the lepton asymmetry. We will only consider the case when the asymmetries in all active species (ν_e, e_L, e_R, ν_μ, μ_L, μ_R, ν_τ, τ_L, τ_R) are equal. Strictly speaking, this is not satisfied in the νMSM, since the generation of lepton asymmetries takes place when the reactions changing neutrino flavours freeze out [1]. We make this assumption in order to keep the discussion as simple as possible, and also because it yields the most conservative constraints, leading to the largest sterile neutrino abundance and consequently weakening the X-ray bounds. We discuss the general formalism applicable in this setting in Sec. 2.1.

At the same time, there is no reservoir replenishing the lepton asymmetry if a part of it is converted to right-handed neutrinos: the CP-violating reactions generating the asymmetry cease to take place at temperatures above a few GeV [1]. Together with the third assumption this completely fixes the time evolution of the lepton asymmetry; this will be demonstrated in Sec. 2.2.

The fourth and final assumption asserts that the density of the right-handed neutrinos produced is below its equilibrium value. This assumption is necessary for the validity of the quantum field theoretic formulation of refs. [11, 12]; on the other hand, it may be violated in certain parts of the parameter space. In Sec. 2.3 we outline a phenomenological way to correct for a possible violation.

2.1. Results in terms of a generic lepton asymmetry

Under the assumption of a chemically equilibrated lepton asymmetry among the active species, the formal determination of the sterile neutrino production rate proceeds almost

exactly as in ref. [11], with the only difference that the density matrix of the Minimal Standard Model (MSM) now takes the form[3]

$$\hat{\rho}_{\rm MSM} = Z_{\rm MSM}^{-1} \exp[-\beta(\hat{H}_{\rm MSM} - \mu_L \hat{L}_{\rm MSM})] \; . \tag{2.2}$$

Here $\beta \equiv 1/T$; $\mu_L \neq 0$ unlike in ref. [11]; and $\hat{L}_{\rm MSM}$ is the total lepton number operator within the MSM,

$$\hat{L}_{\rm MSM} \equiv \int {\rm d}^3\mathbf{x} \sum_{\alpha=e,\mu,\tau} \left[\hat{\bar{l}}_{\alpha L} \, \gamma_0 \, \hat{l}_{\alpha L} + \hat{\bar{l}}_{\alpha R} \, \gamma_0 \, \hat{l}_{\alpha R} + \hat{\bar{\nu}}_{\alpha L} \, \gamma_0 \, \hat{\nu}_{\alpha L} \right] \; , \tag{2.3}$$

with $l_e \equiv e, l_\mu \equiv \mu, l_\tau \equiv \tau$; and $\hat{\psi}_L \equiv a_L \hat{\psi}$, $\hat{\psi}_R \equiv a_R \hat{\psi}$.

According to ref. [11], the phase space density $f_1(t, \mathbf{q})$ of right-handed neutrinos in either helicity state s,

$$f_1(t, \mathbf{q}) \equiv \sum_{s=1,2} \frac{{\rm d}N_1^{(s)}(t, \mathbf{x}, \mathbf{q})}{{\rm d}^3\mathbf{x} \, {\rm d}^3\mathbf{q}} \; , \tag{2.4}$$

obeys the equation

$$\left(\frac{\partial}{\partial t} - H q_i \frac{\partial}{\partial q_i} \right) f_1(t, \mathbf{q}) = R(T, \mathbf{q}) \; . \tag{2.5}$$

Here H is the Hubble parameter, $H = {\rm d}\ln a(t)/{\rm d}t$, and q_i are the spatial components of the physical momentum $\mathbf{q}$, defined in a local Minkowskian frame. Repeating the analysis of ref. [11] with $\mu_L \neq 0$, the source term reads

$$R(T, \mathbf{q}) = \frac{1}{(2\pi)^3 q^0} \sum_{\alpha=1}^{3} |M_D|^2_{\alpha 1} {\rm Tr} \left\{ \not{Q} \, a_L \Big[n_{\rm F}(q^0 - \mu_L) \rho_{\alpha\alpha}(Q) + n_{\rm F}(q^0 + \mu_L) \rho_{\alpha\alpha}(-Q) \Big] a_R \right\} \; , \tag{2.6}$$

where $n_{\rm F}(q) \equiv 1/[\exp(q/T)+1]$ is the Fermi distribution function; $\rho_{\alpha\alpha}$ is the spectral function related to the propagator of the active neutrino of generation α; and Q is the on-shell four-momentum of the right-handed neutrino, i.e. $Q^2 = M_1^2$. Noting that the solution of Eq. (2.5) only depends on $q \equiv |\mathbf{q}|$, it can be written as [12]

$$f_1(t_0, q) = \int_{T_0}^{\infty} \frac{{\rm d}T}{T^3} \, \frac{M_0(T)}{3 c_s^2(T)} R\left(T, q \frac{T}{T_0} \left[\frac{h_{\rm eff}(T)}{h_{\rm eff}(T_0)} \right]^{\frac{1}{3}} \right) \; , \tag{2.7}$$

where $M_0(T) \equiv M_{\rm Pl} \sqrt{45/4\pi^3 g_{\rm eff}(T)}$; $g_{\rm eff}(T)$ parametrizes the energy density e as $e \equiv \pi^2 T^4 g_{\rm eff}(T)/30$; and $h_{\rm eff}(T)$ parametrizes the entropy density s as $s \equiv 2\pi^2 T^3 h_{\rm eff}(T)/45$. Moreover, c_s^2 is the sound speed squared, given by $1/c_s^2(T) = 3 + T h'_{\rm eff}(T)/h_{\rm eff}(T)$. Note that in Eq. (2.7), the chemical potential μ_L may be taken to depend on T in any way, to be specified later on from physical considerations.

[3] In general, different chemical potentials have to be introduced for different leptonic flavours.

To derive an expression for $\rho_{\alpha\alpha}$, we follow the steps in Sec. 3.2 of ref. [11], but without assuming anything about the symmetry properties of the active neutrino self-energy for the moment. The Euclidean propagator (cf. Eq. (3.10) of ref. [11]) then becomes

$$\Pi^E_{\alpha\alpha}(\tilde{Q}) = a_L \frac{1}{-i\tilde{\not{Q}} + i\tilde{\not{\Sigma}}(-\tilde{Q})} a_R = a_L \frac{i\tilde{\not{Q}} - i\tilde{\not{\Sigma}}(-\tilde{Q})}{[\tilde{Q} - \tilde{\Sigma}(-\tilde{Q})]^2} a_R \, . \tag{2.8}$$

We have left out the flavour indices from the active neutrino self-energy $\tilde{\Sigma}$ to compactify the notation somewhat, and the tildes are a reminder of Euclidean conventions.

Carrying out the Wick rotation, we can transform Eq. (2.8) into a retarded Minkowskian propagator (cf. Eq. (3.11) of ref. [11]):

$$\Pi^R_{\alpha\alpha}(q^0, \mathbf{q}) = \Pi^E_{\alpha\alpha}(-iq^0, \mathbf{q}) = a_L \frac{-\not{Q} + \not{\Sigma}(-Q)}{Q^2 - 2Q\cdot\Sigma(-Q) + \Sigma^2(-Q)} a_R \, . \tag{2.9}$$

Writing finally $\Sigma(q^0 \pm i0^+, \mathbf{q}) \equiv \mathrm{Re}\,\Sigma(Q) \pm i\,\mathrm{Im}\,\Sigma(Q)$ and correspondingly $\Sigma(-[q^0 \pm i0^+], -\mathbf{q}) = \mathrm{Re}\,\Sigma(-Q) \mp i\,\mathrm{Im}\,\Sigma(-Q)$, allows to obtain (cf. Eqs. (3.1), (3.4) of ref. [11])

$$\begin{aligned} \rho_{\alpha\alpha}(Q) &= \frac{1}{2i}\Big[\Pi^R_{\alpha\alpha}(q^0 + i0^+, \mathbf{q}) - \Pi^R_{\alpha\alpha}(q^0 - i0^+, \mathbf{q})\Big] & (2.10) \\ &= a_L \frac{-S_I(-Q)[\not{Q} - \mathrm{Re}\,\not{\Sigma}(-Q)] - S_R(-Q)\,\mathrm{Im}\,\not{\Sigma}(-Q)}{S_R^2(-Q) + S_I^2(-Q)} a_R \, , & (2.11) \end{aligned}$$

where

$$\begin{aligned} S_R(-Q) &\equiv [Q - \mathrm{Re}\,\Sigma(-Q)]^2 - [\mathrm{Im}\,\Sigma(-Q)]^2 \, , & (2.12) \\ S_I(-Q) &\equiv -2[Q - \mathrm{Re}\,\Sigma(-Q)]\cdot \mathrm{Im}\,\Sigma(-Q) \, . & (2.13) \end{aligned}$$

These expressions can trivially be written also for $\rho_{\alpha\alpha}(-Q)$, and the results can then be inserted into Eq. (2.6). The outcome constitutes a generalization of Eq. (3.12) of ref. [11].

To compactify the resulting equations somewhat, we make the following simplifications. We note, first of all, that in the imaginary part $\mathrm{Im}\,\Sigma$, the chemical potential changes the thermal distribution functions of the on-shell leptons that appear in the intermediate states. Given that we are interested in the case $\mu_L/T \ll 1.0$, however, these changes are not important, and will be ignored in the following. Then we can assume that $\mathrm{Im}\,\Sigma$ does not get modified by μ_L and, in particular, that $\mathrm{Im}\,\Sigma(-Q) = \mathrm{Im}\,\Sigma(Q)$, as is the case for $\mu_L = 0$.

As far as $\mathrm{Re}\,\Sigma$ is concerned, we note that its general structure can be written as

$$\mathrm{Re}\,\not{\Sigma}_{\alpha\alpha}(Q) = \not{Q}\, a_{\alpha\alpha}(Q) + \not{u}\, b_{\alpha\alpha}(Q) + \not{u}\, c_{\alpha\alpha}(Q) \, , \tag{2.14}$$

where $u = (1, \mathbf{0})$. We note that the function $a_{\alpha\alpha}(Q)$ can be ignored, since it is small compared with the tree-level term $\not{Q}$. On the other hand the latter structures in Eq. (2.14) do not appear at tree-level, and need to be kept. We have separated two terms: a function $b_{\alpha\alpha}(Q)$ odd in Q, appearing already in the charge symmetric situation, as well as a function $c_{\alpha\alpha}(Q)$, defined to

be even in Q. The function $c_{\alpha\alpha}(Q)$ must be proportional to the leptonic chemical potential (or leptonic net number densities), and it is this function which plays an essential role in the following. The explicit expression for $c_{\alpha\alpha}(Q)$ can be extracted from ref. [48]; for $q^0 \ll m_W$, we can work to first order in an expansion in $1/m_W^2$, and then the result reads

$$c_{\alpha\alpha} = 3\sqrt{2}G_F(1 + 4\sin^2\theta_{\rm W})n_{\nu_e} \,, \tag{2.15}$$

where $G_F = g_w^2/4\sqrt{2}m_W^2$ is the Fermi constant and, as mentioned, we assumed that all active leptonic densities are equal: $n_{\nu_e} = n_{e_L} = n_{e_R} = n_{\mu_L} = ...$.[4]

With these simplifications, we can write

$$\not{Q} + \mathrm{Re}\,\not{\Sigma}\,(Q) \approx \not{Q} + \not{u}\,(b+c) \,, \tag{2.16}$$

$$\Big[Q + \mathrm{Re}\,\Sigma(Q)\Big]^2 \approx M_1^2 + 2q^0(b+c) + (b+c)^2 \,, \tag{2.17}$$

$$\not{Q} - \mathrm{Re}\,\not{\Sigma}\,(-Q) \approx \not{Q} + \not{u}\,(b-c) \,, \tag{2.18}$$

$$\Big[Q - \mathrm{Re}\,\Sigma(-Q)\Big]^2 \approx M_1^2 + 2q^0(b-c) + (b-c)^2 \,, \tag{2.19}$$

where $b \equiv b_{\alpha\alpha}(Q)$, $c \equiv c_{\alpha\alpha}(Q)$. Furthermore, all appearances of $\mathrm{Im}\,\Sigma$ can be written in terms of the objects

$$I_Q \equiv \mathrm{Tr}\Big[\not{Q}\, a_L\, \mathrm{Im}\,\not{\Sigma}\,(Q) a_R\Big] = 2\, Q\cdot \mathrm{Im}\,\Sigma(Q) \,, \tag{2.20}$$

$$I_u \equiv \mathrm{Tr}\Big[\not{u}\, a_L\, \mathrm{Im}\,\not{\Sigma}\,(Q) a_R\Big] = 2\, u\cdot \mathrm{Im}\,\Sigma(Q) \,. \tag{2.21}$$

Note, in particular, that $\mathrm{Im}\,\not{\Sigma}$ has a structure analogous to Eq. (2.14), with one term proportional to $\not{Q}$ and another to $\not{u}$, and that consequently even $[\mathrm{Im}\,\Sigma]^2$ can be written in terms of the structures in Eqs. (2.20), (2.21), as

$$\Big[\mathrm{Im}\,\Sigma(Q)\Big]^2 = \frac{-I_Q^2 + 2q^0 I_Q I_u - M_1^2 I_u^2}{4\mathbf{q}^2} \,. \tag{2.22}$$

Inserting these simplifications into Eqs. (2.6), (2.11)–(2.13), we finally obtain

$$R(T,q) \approx \frac{1}{(2\pi)^3 q^0} \sum_{\alpha=e,\mu,\tau} |M_D|^2_{\alpha 1} \times$$
$$\times \left\{ n_{\rm F}(q^0+\mu_L) \frac{2S_I(Q)[M_1^2 + q^0(b+c)] - S_R(Q) I_Q}{S_R^2(Q) + S_I^2(Q)} + (c \to -c, \mu_L \to -\mu_L) \right\} \,, \tag{2.23}$$

where

$$S_R(Q) = M_1^2 + 2q^0(b+c) + (b+c)^2 + \frac{I_Q^2 - 2q^0 I_Q I_u + M_1^2 I_u^2}{4\mathbf{q}^2} \,, \tag{2.24}$$

$$S_I(Q) = I_Q + (b+c) I_u \,. \tag{2.25}$$

[4] In general, $c_{\alpha\alpha} = \sqrt{2}G_F[(1+2x_{\rm W})n_{l_{\alpha L}} - (1-2x_{\rm W})\sum_{\beta\neq\alpha} n_{l_{\beta L}} + 2x_{\rm W}\sum_\beta n_{l_{\beta R}} + 2n_{\nu_\alpha} + \sum_{\beta\neq\alpha} n_{\nu_\beta}]$, where $x_{\rm W} \equiv \sin^2\theta_{\rm W}$.

We remark that the production of the dark matter sterile neutrinos, with masses in the keV range, takes place at temperatures below a few GeV (cf. Fig. 2 below). In this case, like already at $\mu_L = 0$, it is numerically a very good approximation to set the term I_u to zero, whereby Eqs. (2.24), (2.25) simplify further.

Although the formulae given are valid beyond perturbation theory, a practical application does make use of approximate perturbative expressions for the functions b, c and I_Q. It is important to realise that at the point of a resonance, where some of the "large" terms ($M_1^2 + 2q^0 b$ and $\pm 2q^0 c$) cancel against each other, the magnitude of the remainder is determined by higher order terms ($(b \pm c)^2$ and I_Q). A consistent treatment to a certain order in perturbation theory would hence require a correspondingly precise (2-loop) determination of the large terms $2q^0 b, 2q^0 c$. At the same time, in a practical application we are not sitting precisely at the point of a resonance, but integrate over its contribution, so that for instance a slight misplacement of the precise temperature at which the resonance takes place plays little role. Consequently, we continue to use 1-loop expressions for the functions b and c throughout[5]. Nevertheless, as we will see, the fact that at the point of the resonance, $\mathrm{Im}\,\Sigma$ plays a role also in the denominator, will imply that a large $\mathrm{Im}\,\Sigma$ can also lead to a decreased abundance, in contrast to the case of non-resonant production, where $\mathrm{Im}\,\Sigma$ essentially only plays a role in the numerator. For a recent discussion of various resonance-related phenomena, see ref. [49].

To be more quantitative about the role of the resonance, we can work out its contribution to the production rate semi-analytically. To a good approximation, the resonance is at the point where the function

$$\mathcal{F}(T) \equiv M_1^2 + 2q^0(b - c) \tag{2.26}$$

vanishes (this comes from the latter term in Eq. (2.23), after the insertion of Eq. (2.24)). Around this point, the production rate in Eq. (2.23) can be approximated as

$$R(T,q) \approx \frac{n_{\mathrm{F}}(q^0 - \mu_L)}{(2\pi)^3 q^0} \sum_{\alpha=e,\mu,\tau} |M_D|^2_{\alpha 1} [M_1^2 + q^0(b-c)] \frac{2I_Q}{\mathcal{F}^2(T) + I_Q^2} \tag{2.27}$$

$$\approx \frac{n_{\mathrm{F}}(q^0 - \mu_L)}{(2\pi)^2 2q^0} \sum_{\alpha=e,\mu,\tau} |M_D|^2_{\alpha 1}\, M_1^2\, \delta(\mathcal{F}(T)) \;, \tag{2.28}$$

where we made use of the fact that I_Q is very small, in order to identify a representation of the Dirac delta-function. Inspecting the expressions for b and c, the function $\mathcal{F}$ is positive at very low temperatures (because M_1^2 dominates) and at very large temperatures (because b dominates), but for sufficiently large n_{ν_e}/s and sufficiently small q/T, the term c overtakes the others at intermediate temperatures; there are then two zeros of $\mathcal{F}$, and it turns out to be the lower among these that gives the dominant contribution. We denote the corresponding temperature by T_R. Eq. (2.7) can now be integrated, to yield

$$f_1(t_0, q) \approx \sum_{\alpha=e,\mu,\tau} |M_D|^2_{\alpha 1}\, \frac{1}{T_R^3} \frac{M_0(T_R)}{3c_s^2(T_R)} \frac{n_{\mathrm{F}}(q^0 - \mu_L)}{(2\pi)^2 2q^0} \frac{M_1^2}{|\mathcal{F}'(T_R)|}\bigg|_{\mathcal{F}(T_R)=0} \;. \tag{2.29}$$

[5]For all quantities not specified explicitly in this section, we use the expressions given in ref. [11].

2.2. Time evolution of the lepton asymmetry

The main formula of the previous section, Eq. (2.23), depends on the leptonic chemical potential, μ_L, and on the lepton asymmetry, n_{ν_e}, the two of which are related through Eq. (A.3). However, the dependence of these quantities on the time (or temperature) has been left open. We now need to insert further physical input in order to fix this dependence.

It is important to realize, first of all, that no reservoir exists for the lepton asymmetry: as explained in ref. [1], the lepton asymmetry was generated by CP-violating processes active at temperatures around a few GeV, which subsequently ceased to operate.

Second, the mass of the lightest right-handed neutrino, M_1, is much below the temperature, $M_1 \ll T$. Therefore lepton asymmetry violating processes, whose rate is proportional to M_1^2, can to a very good approximation be neglected. In other words, dark matter sterile neutrinos and the active leptons can be characterized by a conserved quantity, which we may call the total lepton number. In fact, this physics is effectively already built in in Eq. (2.6), which shows that the rate for generating any of the two sterile neutrino states is a sum of two terms, with opposite chemical potentials appearing in them, as is appropriate for "particles" and "anti-particles".

As a result of these two facts, the resonant transitions from active to sterile neutrinos, or more precisely the C-odd part of Eq. (2.6), cause the original asymmetry to get *depleted*. If the resonance is very effective, the depletion is fast and thereby rapidly terminates the resonance phenomenon.

To be more quantitative, we make the (optimistic) assumption that the flavour and chirality changing processes within the active generations are fast enough to stay in thermal equilibrium. There is then a reservoir of nine spin-1/2 degrees of freedom (three generations, each with left-handed neutrinos and both-handed charged leptons) converting to sterile neutrinos. Denoting the two terms in Eq. (2.6) by R_- and R_+, respectively, Eq. (2.5) can then be split and subsequently completed into a closed set of three equations (we also adopt an ansatz removing the terms proportional to the Hubble parameter from Eq. (2.5)):

$$\frac{\mathrm{d}}{\mathrm{d}t} f_-\Big(t, q(t_0)\frac{a(t_0)}{a(t)}\Big) = R_-\Big(T, q(t_0)\frac{a(t_0)}{a(t)}\Big)\,, \tag{2.30}$$

$$\frac{\mathrm{d}}{\mathrm{d}t} f_+\Big(t, q(t_0)\frac{a(t_0)}{a(t)}\Big) = R_+\Big(T, q(t_0)\frac{a(t_0)}{a(t)}\Big)\,, \tag{2.31}$$

$$\frac{\mathrm{d}}{\mathrm{d}t}\Big\{9\, a^3(t) n_{\nu_e}(t)\Big\} = a^3(t)\int \mathrm{d}^3\mathbf{q}\,\Big[R_+(T,q) - R_-(T,q)\Big]\,, \tag{2.32}$$

where the dark matter spectrum f_1 is now represented by the sum $f_1(T,q) = f_-(T,q) + f_+(T,q)$. The structure of these equations is such that the total lepton charge in a comoving volume,

$$L_{\mathrm{tot}} \equiv a^3(t)\Big\{9\, n_{\nu_e}(t) + \int \mathrm{d}^3\mathbf{q}\,\Big[f_-(t,q) - f_+(t,q)\Big]\Big\}\,, \tag{2.33}$$

indeed remains conserved, as must be the case for $M_1 \to 0$.

Note that within the approximation of Eq. (2.28), the term R_+ could be omitted from Eqs. (2.30)–(2.32), which would simplify the system somewhat. Another practical simplification is to solve the equations in terms of the temperature rather than the time, as we already did in Eq. (2.7).

A rough estimate for when the depletion has a substantial impact can be obtained as follows. If *all* of the original lepton asymmetry converts to sterile neutrinos, then $n_1/s \geq 9n_{\nu_e}/s$, where s is the total entropy density, and

$$n_1(t_0) \equiv \int \mathrm{d}^3\mathbf{q}\, f_1(t_0, \mathbf{q}) \; . \tag{2.34}$$

Therefore the depletion is substantial if $n_{\nu_e}/s \lesssim n_1/9s$. Evaluating the right-hand side of this inequality for the case that sterile neutrinos account for all of dark matter, Eq. (3.3), we get $n_{\nu_e}/s \lesssim 4.0 \times 10^{-4} \times \mathrm{keV}/9M_1$, i.e.

$$\frac{M_1}{\mathrm{keV}} \lesssim 45 \left(10^6 \frac{n_{\nu_e}}{s}\right)^{-1} . \tag{2.35}$$

In other words, for a small initial asymmetry, the depletion has a significant impact at all the masses, while for a large initial asymmetry, the effect of the depletion is subdominant (because there is more to deplete), unless the mass is small.

2.3. Back reaction and equilibration

The derivation of the formulae that our work is based upon, Eqs. (2.30)–(2.32), contains the assumption that the particles produced do not thermalize, i.e., that their density remains below the equilibrium value at all times. Let us investigate the validity of this assumption.

It is relatively easy to establish that the *total* number density of the sterile neutrinos produced does remain significantly below the equilibrium value. Indeed, the density of the sterile neutrinos is constrained from above by Eq. (3.3), and consequently

$$\begin{aligned} \frac{n_1(T_0)}{n_{\mathrm{eq}}(T_0)} &\lesssim 4.0 \times 10^{-4} \frac{s(T_0)}{n_{\mathrm{eq}}(T_0)} \frac{\mathrm{keV}}{M_1} \approx 9.64 \times 10^{-4}\, h_{\mathrm{eff}}(T_0)\, \frac{\mathrm{keV}}{M_1} \\ &\lesssim 0.072\, \frac{\mathrm{keV}}{M_1} \, , \end{aligned} \tag{2.36}$$

where we inserted $n_{\mathrm{eq}}(T_0) = 3\zeta(3)T_0^3/2\pi^2$ (cf. Eq. (A.4)) as well as $h_{\mathrm{eff}}(T_0) \lesssim 75$ corresponding to $T_0 \lesssim 1$ GeV [50]. Thereby the lightest sterile neutrinos appear indeed to be out of equilibrium in the whole range $M_1/\mathrm{keV} \geq 0.1$ that we are interested in.

It must be realized, however, that the inequality (2.36) is not sufficient to guarantee the absence of problems. Indeed, the spectrum of the sterile neutrinos produced is strongly tilted towards the infrared [2, 7]. Given that we are considering fermions, it must then be checked that the Pauli exclusion principle is not violated at small momenta. Although an exact quantum field theoretic treatment would guarantee this automatically, the assumption of a

non-thermal result in the derivation of Eq. (2.23) means that this consideration now enters as an additional ingredient. We refer to the dynamics that prevents an excessive growth of the fermionic density at small momenta as "back reaction".

Motivated by Boltzmann equations, and recalling our normalization (cf. Eq. (2.4)), we expect that the way that back reaction works is to modify the source terms for the distribution functions f_-, f_+ (cf. Eqs. (2.6), (2.30), (2.31)) by replacing

$$\frac{n_{\rm F}(q^0-\mu_L)}{(2\pi)^3} \to \frac{n_{\rm F}(q^0-\mu_L)}{(2\pi)^3} - f_- \,, \quad \frac{n_{\rm F}(q^0+\mu_L)}{(2\pi)^3} \to \frac{n_{\rm F}(q^0+\mu_L)}{(2\pi)^3} - f_+ \,. \tag{2.37}$$

However, since this recipe would be purely phenomenological at this stage, and since the resulting equations are quite difficult to solve numerically[6], we follow a simpler approach in the following. Indeed, we first solve Eqs. (2.30)–(2.32) without back reaction, yielding the distribution functions which we denote by $f_-^{(0)}$, $f_+^{(0)}$. Subsequently, we construct the approximants

$$f_\mp \simeq \frac{\frac{n_{\rm F}(q^0\mp\mu_L)}{(2\pi)^3}\cdot f_\mp^{(0)}}{\frac{n_{\rm F}(q^0\mp\mu_L)}{(2\pi)^3} + f_\mp^{(0)}} \,. \tag{2.38}$$

This amounts to a rough iterative solution of the structures suggested by Eq. (2.37); guarantees that $f_\mp$ never exceed the equilibrium distributions $n_{\rm F}(q^0\mp\mu_L)/(2\pi)^3$; and, for $f_\mp \ll n_{\rm F}(q^0\mp\mu_L)/(2\pi)^3$, yields the correct result $f_\mp = f_\mp^{(0)}$.

In order to estimate the practical importance of the back reaction, we have determined our main observables (cf. Secs. 3, 4) for a number of parameter values both from $f_\mp^{(0)}$ and $f_\mp$. We return to the corresponding error estimates in connection with the numerical data.

3. Sterile neutrino abundance

The task now is to evaluate the integral in Eq. (2.7), with the lepton asymmetry evolved according to Eq. (2.32), producing the distribution function $f_1(t_0, q)$, with $q \equiv |\mathbf{q}|$; and then to integrate over $\mathbf{q}$, to get the total number density n_1 (the order of the integrations over T and q can of course be interchanged). We choose t_0 to be the time corresponding to $T_0 = 1$ MeV, below which active neutrinos start to decouple. In order to present the numerical results, we start by introducing some further notation.

First of all, it is conventional to express the mixing angle as $\sin^2 2\theta_{\alpha 1}$. For the very small Yukawa couplings that we are interested in, it is an excellent approximation to write

$$\sin^2 2\theta_{\alpha 1} = 4\theta_{\alpha 1}^2 = 4\frac{|M_D|_{\alpha 1}^2}{M_1^2} \,. \tag{3.1}$$

[6]If the spectra $f_\mp$ do *not* appear in $R_\mp$ on the right-hand side, we can integrate over momenta in Eqs. (2.30), (2.31), to obtain a coupled set of ordinary differential equations for integrated densities; on the contrary, if the spectra *do* appear in $R_\mp$ on the right-hand side, modes with different momenta q couple to each other and need to be solved simultaneously, which makes the problem significantly harder.

Second, we introduce a total mixing angle as

$$\sin^2 2\theta \equiv \sum_{\alpha=e,\mu,\tau} 4\theta_{\alpha 1}^2 \,, \tag{3.2}$$

which is the quantity appearing in the X-ray constraints to be discussed below (cf. Fig. 4).

Now, we can write the total right-handed neutrino density as $n_1(t_0) \equiv \sum_{\alpha=e,\mu,\tau} n_{\alpha 1}(t_0)$, where $n_{\alpha 1}$ is the contribution from active flavour α to the dark matter abundance. This contribution can conveniently be characterized through the yield parameter $Y_{\alpha 1} \equiv n_{\alpha 1}/s$. The corresponding relative energy fraction is $\Omega_{\alpha 1} \equiv M_1 n_{\alpha 1}/\rho_{\rm cr} = M_1 Y_{\alpha 1}/(\rho_{\rm cr}/s)$. Inserting $\rho_{\rm cr}/s \approx 3.65 \times 10^{-9} h^2\,{\rm GeV}$ from Particle Data Group [45], and noting that $\Omega_{\alpha 1} h^2$ can amount to at most the experimentally known dark-matter density, $\Omega_{\rm dm} h^2 = 0.1143 \pm 0.0034$ (68% CL) [46], we obtain an upper bound on $Y_{\alpha 1}$:

$$Y_{\alpha 1} \lesssim 4.0 \times 10^{-4} \times \frac{\rm keV}{M_1} \,. \tag{3.3}$$

Since $Y_{\alpha 1}$ depends monotonously (though non-linearly, because of the depletion discussed in Sec. 2.2) on $\sin^2 2\theta_{\alpha 1}$, this equation yields an upper bound on the mixing angle.

Following ref. [12], we concentrate particularly on two flavour structures. In the non-resonant case, for a fixed mixing angle, a hierarchy $Y_{e1} > Y_{\mu 1} > Y_{\tau 1}$ can be observed [12], because heavier scatterers suppress the production rate. The largest abundance, and the most stringent upper bound on $\sin^2 2\theta$, is then obtained with

$$|M_D|_{e1} \neq 0 \,, \quad |M_D|_{\mu 1} = |M_D|_{\tau 1} = 0 \qquad\qquad \text{“case 1”} \,, \tag{3.4}$$

while the smallest relic abundance and the weakest upper bound on $\sin^2 2\theta$ is obtained when

$$|M_D|_{\tau 1} \neq 0 \,, \quad |M_D|_{e1} = |M_D|_{\mu 1} = 0 \qquad\qquad \text{“case 2”} \,. \tag{3.5}$$

As already mentioned, in the resonant case the roles of what leads to the strongest and weakest upper bound may get interchanged, because the structure of Eq. (2.23) is fairly complicated, but it appears that these two cases should still capture the most extreme possibilities.

To integrate Eqs. (2.7), (2.32) in practice, we set the upper limit of the T-integration to $T_{\rm max} = 4$ GeV where $R(T,q)$ is vanishingly small, and the lower limit to $T_0 = 1$ MeV. We first integrate over q, and then evolve $n_{\alpha 1}$, $Y_{\alpha 1}$ and n_{ν_e}/s through coupled ordinary differential equations in T. This is repeated with several $\sin^2 2\theta$ in order to find the value satisfying the constraint in Eq. (3.3). Our numerical implementation follows that in ref. [12]. In particular, as mentioned above, $\mathrm{Im}\,\Sigma$ can be evaluated just as in the case without a lepton asymmetry. At the same time, the existence of a narrow resonance does make the integrations over q and T much more demanding than in the charge-symmetric case; most importantly, the resolution in the q-direction needs to be significantly increased.

We also remark that at small M_1/keV and large asymmetries, a direct numerical integration becomes increasingly difficult, but at the same time Eq. (2.29) becomes more accurate.

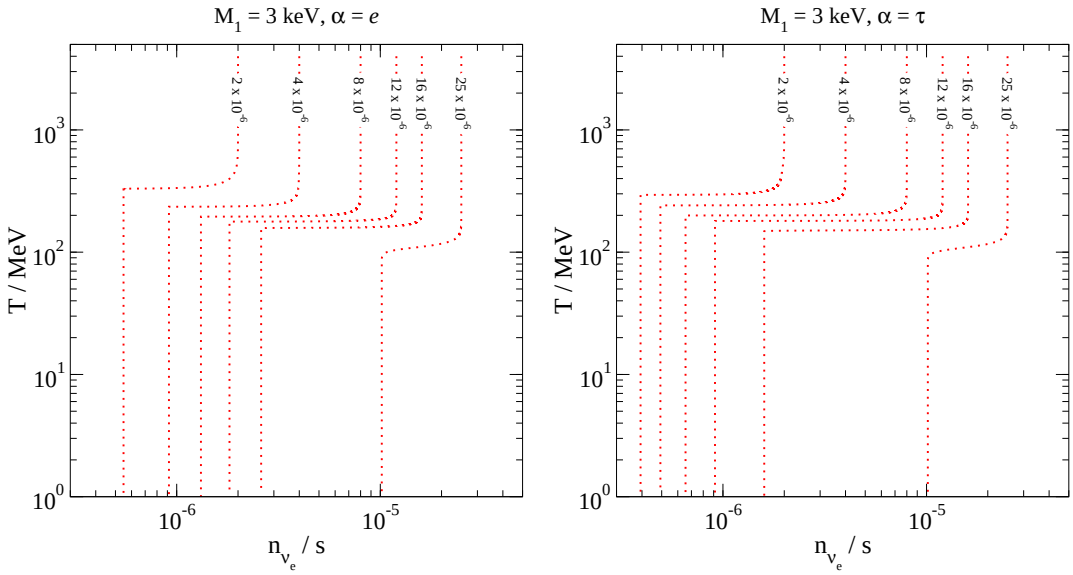

Figure 1: Examples of the T-evolution of the lepton asymmetry n_{ν_e}/s (cf. Sec. 2.2), for a fixed $M_1 = 3$ keV. Left: $\alpha = e$. Right: $\alpha = \tau$. Note that our results differ even qualitatively from ref. [14] where the asymmetry crosses zero at some temperature.

However, the asymmetry gets rapidly depleted in this regime, so that in fact Eq. (2.29) is a good approximation only at the early stages of the resonance. We have found that a workable method is to approximate R as a sum of a C-odd and C-even part; the C-odd part is approximated by Eq. (2.29), while the C-even part, which dominates for small asymmetries, is approximated by the full R from ref. [12], with μ_L equal to zero. We have checked that the results obtained this way extrapolate, within our resolution, to the "exact" results which can be reliably determined at large masses, $M_1 \gtrsim 10$ keV.

In Fig. 1 we show examples of the evolution of the lepton asymmetry for various initial values. It can be observed that the resonance is quite narrow, and quite effective; in particular, for $n_{\nu_e}/s \lesssim 10^{-6}$, most of the initial lepton asymmetry is rapidly converted to sterile neutrinos, so that the resonance becomes ineffective. Sterile neutrinos are then dominantly produced thermally, like in ref. [12], and the mixing angle needs to be large. If the lepton asymmetry reservoir were smaller, for instance with three components rather than nine, then the depletion would be even more rapid.

In Fig. 2 we show the resonance temperatures (where existent) for two momenta and various asymmetries, as a function of the mass M_1. We note that for M_1 of a few keV, the production peaks at temperatures very close to the QCD crossover. This introduces severe hadronic uncertainties to the results, as will be discussed below.

In Fig. 3 we show the upper bound on the mixing angle following from Eq. (3.3), for $n_{\nu_e}/s = 16.3 \times 10^{-6}$. This value has been chosen in order to allow for a comparison with fig. 1 of ref. [51]. It can be seen that at large masses, $M_1 \gtrsim 3$ keV, the general order of

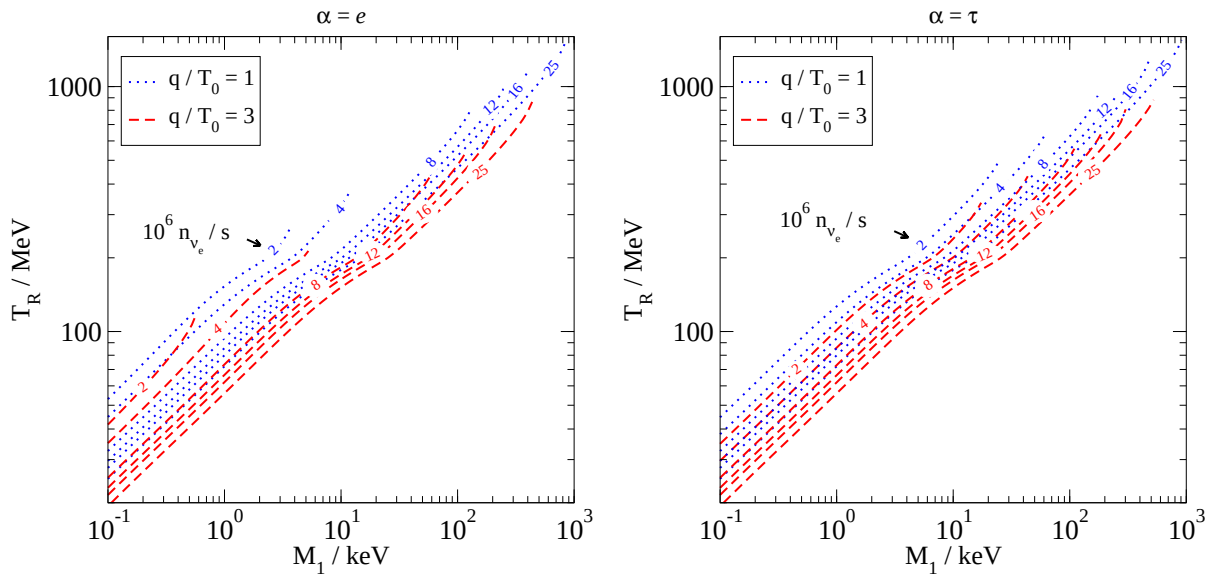

Figure 2: The resonance temperature corresponding to Eq. (2.29), for the modes $q/T_0 = 1$ and $q/T_0 = 3$, with $T_0 = 1$ MeV. Left: $\alpha = e$. Right: $\alpha = \tau$. It is seen that, for a given M_1, the resonance first affects the smallest values of q/T_0, and that the resonance extends to larger M_1 with increasing asymmetry (the asymmetry is indicated in units of $10^6 n_{\nu_e}/s$ on top of the curves).

magnitude of our result is remarkably close to the result of ref. [51], despite the fact that this work was using a simplified kinetic equation and different approximations. On the other hand, at small masses, where the depletion discussed in Sec. 2.2 is effective, the results are dramatically different.

In Fig. 3 we have also considered the effects of two sources of hadronic uncertainties: from the equation-of-state, which is defined to correspond to a 20% rescaling of the pseudocritical temperature of the QCD crossover; and from hadronic scatterings, which is defined to correspond to evaluating the hadronic contributions to the vector and axial current spectral functions with *non-interacting* quarks, and an effective number $N_c = 0$ or $N_c = 3$ of colours. For justification and more details on this phenomenological but nevertheless conservative procedure, we refer to Sec. 5 of ref. [12]. For plotting the dashed and dotted lines in Fig. 3, we have simultaneously set both uncertainties to their maximal values. It is seen that the resulting error depends strongly on parameters, but can be as large as 50%.

The theoretical upper bound from Eq. (3.3) is compared with experimental constraints (from the non-observation of any X-ray sterile neutrino decay peak in various presumed dark matter concentrations) in Fig. 4. A more detailed discussion concerning the implications of Fig. 4 follows in Sec. 5.

Finally, we note that the plots in this section were produced without taking into account the back reaction discussed in Sec. 2.3, i.e., by using the distributions $f_{\mp}^{(0)}$. By recomputing $Y_{\alpha 1}$ for a number of masses and asymmetries from the corrected distributions $f_{\mp}$, we find that the

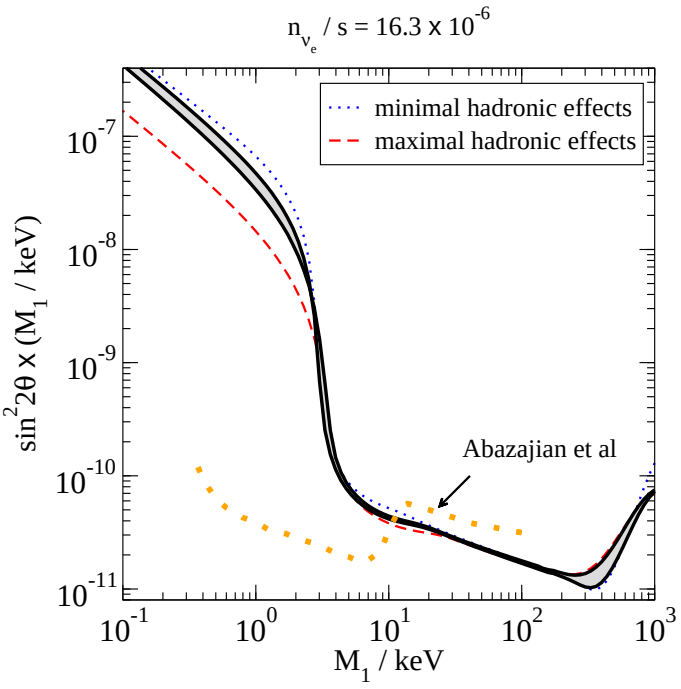

Figure 3: The parameter values that, according to our theoretical computation, lead to the correct dark matter abundance in the Shi-Fuller scenario [2]; if additional sources are present, $\sin^2 2\theta$ must lie *below* the curves shown (cf. Eq. (3.3)). For better visibility, the results have been multiplied by M_1/keV. The grey region between case 1 (lower solid line on the left, upper solid line in the middle and on the right) and case 2 (other solid line) corresponds to different patterns of the active-sterile mixing angles, cf. Eqs. (3.4), (3.5). The dotted and dashed lines correspond to one of these limiting patterns with simultaneously the uncertainties from the equation-of-state and from hadronic scatterings set to their maximal values. The thick dotted line marked with "Abazajian et al" shows the result in Fig. 1 of ref. [51] (the case $L = 0.003$).

errors are maximal, $\sim 25\%$, for small masses, $M_1 \lesssim 3$ keV, and intermediate asymmetries, $n_{\nu_e}/s \sim 10 - 20 \times 10^{-6}$. For larger masses and other asymmetries, the error from the omission of the back reaction is typically below 10%, which we estimate to be well below our other systematic uncertainties.

4. Sterile neutrino spectrum

We now move from the integrated total sterile neutrino abundance, Eq. (2.34), to the momentum distribution function, Eq. (2.7). The physics context where this plays a role is that of structure formation, particularly at the smallest scales (Lyman-α data). The corresponding constraints are considered to be subject to more uncertainties than the X-ray bounds, both as far as direct observational issues are concerned, as well as with regard to

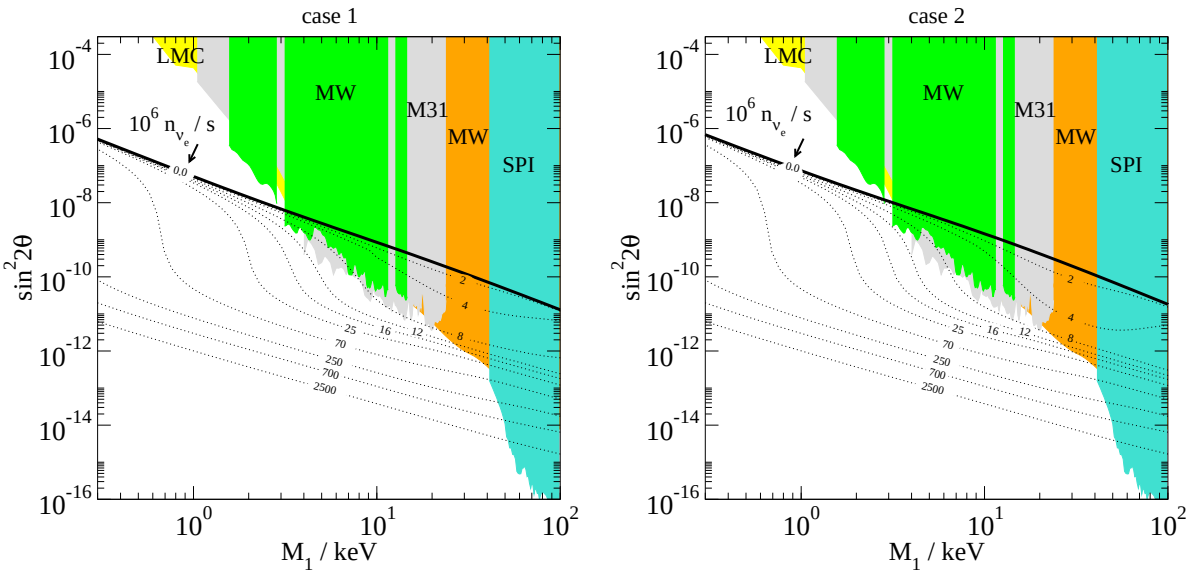

Figure 4: The central region of Fig. 3, $M_1 = 0.3 \ldots 100.0$ keV, compared with regions excluded by various X-ray constraints [22, 25, 30, 31], coming from XMM-Newton observations of the Large Magellanic Cloud (LMC), the Milky Way (MW), and the Andromeda galaxy (M31). SPI marks the constraints from 5 years of observations of the Milky Way galactic center by the SPI spectrometer on board the Integral observatory.

dark matter simulations, which have not been carried out with actual non-equilibrium spectra so far. Nevertheless, adopting a simple recipe for estimating the non-equilibrium effects (cf. Eq. (5.1)), the results of refs. [34, 35] can be re-interpreted as the constraints $M_1 \gtrsim 11.6$ keV and $M_1 \gtrsim 8$ keV, respectively (95% CL), at vanishing asymmetry [12]. Very recently limits stronger by a factor 2–3 have been reported [36]. We return to how the constraints change in the case of a non-zero lepton asymmetry in Sec. 5. We note, however, that the most conservative bound, the so-called Tremaine-Gunn bound [52, 53], is much weaker and reads $M_1 \gtrsim 0.3$ keV [54], which we have chosen as the lower end of the horizontal axes in Figs. 4, 6.

In Fig. 5 we show examples of the spectra, for a relatively small mass $M_1 = 3$ keV (like in Fig. 1), at which point the significant changes caused by the asymmetry can be clearly identified. The general pattern to be observed in Fig. 5 is that for a small asymmetry, the distribution function is boosted only at very small momenta. Quantities like the average momentum $\langle q \rangle_s$ then decrease, as can be seen in Fig. 6. For large asymmetry, the resonance affects all q; the total abundance is strongly enhanced with respect to the case without a resonance, but the shape of the distribution function is less distorted than at small asymmetry, so that the average momentum $\langle q \rangle_s$ returns back towards the value in the non-resonant case. Therefore, for any given mass, we can observe a minimal value of $\langle q \rangle_s$ in Fig. 6, $\langle q \rangle_s \gtrsim 0.3 \langle q \rangle_a$. This minimal value is remarkably independent of M_1, but the value of asymmetry at which

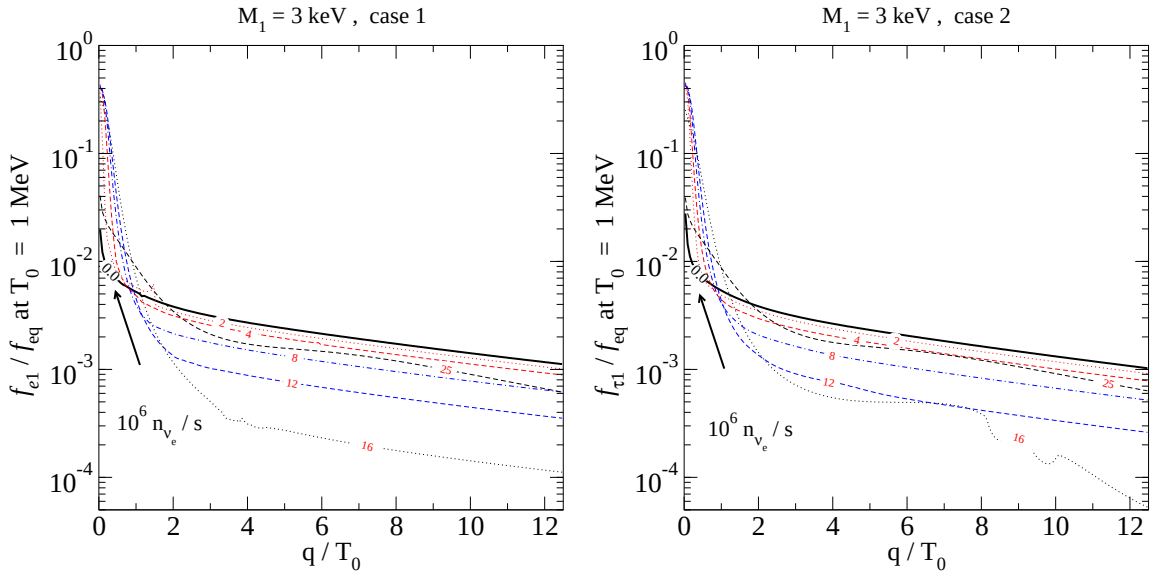

Figure 5: The distribution function $f_{\alpha 1}(t_0, q)$, for $T_0 = 1$ MeV and $M_1 = 3$ keV, normalised to the massless equilibrium value, $f_{\rm eq}(t_0, q) = 2n_{\rm F}(q)/(2\pi)^3$. Left: case 1. Right: case 2. These results can be compared with refs. [2, 7]: the general feature of strong enhancement at small momenta is the same, but our distribution functions show more structure. The case $n_{\nu_e}/s = 16 \times 10^{-6}$ is particularly complicated (and sensitive to uncertainties), since the resonance happens to lie just on top of the QCD crossover, at $T \sim 150 - 200$ MeV, cf. Figs. 1–3.

it is reached decreases with increasing M_1.

Let us stress, however, that the values in Fig. 6 were produced without taking into account the back reaction discussed in Sec. 2.3, i.e., by using the distributions $f_{\mp}^{(0)}$. By recomputing $\langle q\rangle_s/\langle q\rangle_a$ for a number of masses and asymmetries from the approximatively corrected distributions $f_{\mp}$ (shown in Fig. 5), we find that for small masses, $M_1 \lesssim 3$ keV, and intermediate asymmetries, $n_{\nu_e}/s \sim 10 - 20 \times 10^{-6}$, the results in Fig. 6 may be *too small* by up to $\sim 25\%$. Thus, for small masses, the minimal average momentum may be better approximated as $\langle q\rangle_s \gtrsim 0.4\langle q\rangle_a$. For larger masses and other asymmetries, the error from the omission of the back reaction is typically below 10%, which we estimate to be below our other systematic uncertainties.

5. Astrophysical constraints

The purpose of the present section is to combine the results of the previous two sections, and derive the astrophysical constraints that follow from them. Let us start by briefly recapitulating, once more, the two different types of considerations that we have carried out.

First of all, the theoretical computation described in Sec. 3 produces, for a given mass M_1 and mixing angle $\sin^2 2\theta$, a definite total abundance of sterile neutrinos. Requiring that this

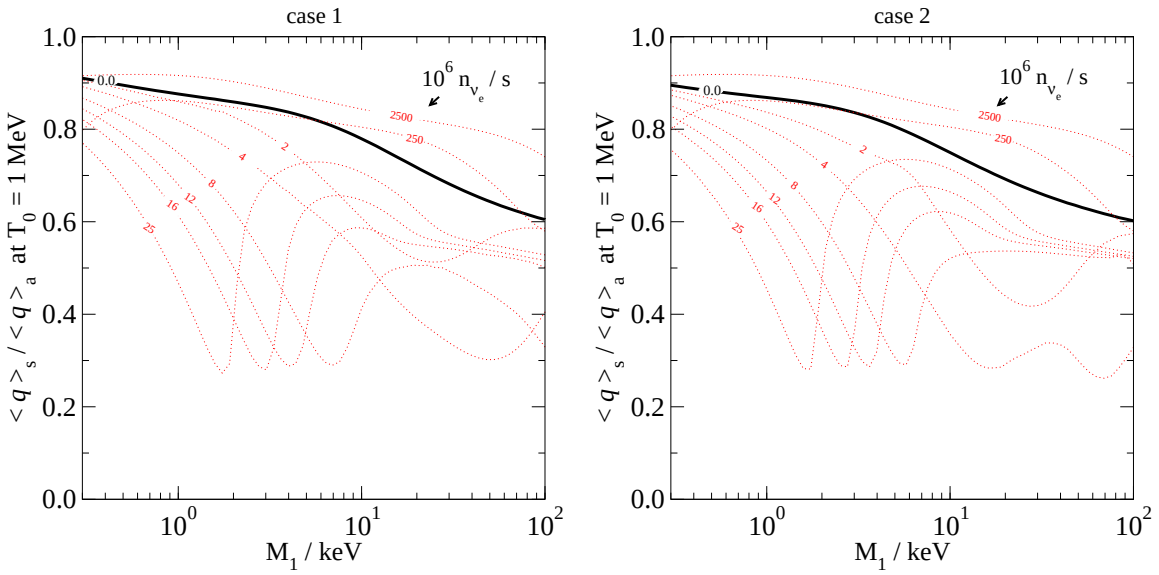

Figure 6: The average sterile neutrino momentum, $\langle q\rangle_s$, normalised to the active neutrino equilibrium value, $\langle q\rangle_a \equiv 7\pi^4 T_0/180\zeta(3) \approx 3.15 T_0$. Left: case 1. Right: case 2.

abundance account for all of the observed energy density in dark matter, leads to the (lepton asymmetry dependent) mass–angle relation shown in Fig. 4.

The most direct constraint on the sterile neutrino dark matter scenario comes from comparing these curves with X-ray observations (Fig. 4). For $n_{\nu_e}/s = 0.0$ we are in the allowed region only for $M_1 \leq 3$ keV. Increasing the asymmetry to $n_{\nu_e}/s \simeq 8\times 10^{-6}$ opens suddenly a whole range of allowed mass values, up to $M_1 \simeq 25$ keV. Increasing the asymmetry further relaxes the upper bound even more but rather slowly; for instance, if the asymmetry is increased to $n_{\nu_e}/s \simeq 25\times 10^{-6}$, then we read from Fig. 4 the upper bound $M_1 \lesssim 40$ keV, while the maximal allowed asymmetry $n_{\nu_e}/s \simeq 2500\times 10^{-6}$ yields the upper bound $M_1 \lesssim 50$ keV.

Another important effect comes from the modification of the sterile neutrino spectrum through a lepton asymmetry. As already found in ref. [2], the non-equilibrium spectrum of the dark matter sterile neutrinos created in the presence of a lepton asymmetry is very different from the thermal one. Some examples are shown in Fig. 5.

Now, an observation of small scale structures in the Lyman-α data puts an upper bound on the free-streaming length and, consequently, on the average velocity of the dark matter particles. This converts to a lower bound on the inverse velocity, which, in the absence of an actual analysis with non-equilibrium spectra, can be roughly estimated as [32]

$$M_1 \frac{\langle q\rangle_a}{\langle q\rangle_s} \gtrsim M_0 \quad \Leftrightarrow \quad M_1 \gtrsim M_0 \frac{\langle q\rangle_s}{\langle q\rangle_a}\,, \tag{5.1}$$

where $\langle q\rangle_a$ and $\langle q\rangle_s$ are the average momenta of active and sterile neutrinos, respectively, at the moment of structure formation, and the value of M_0 is $M_0 \simeq 14$ keV (95% CL) according

to ref. [34] (or $M_0 \simeq 10$ keV at 99.9% CL). According to ref. [35] the bound is somewhat weaker, while according to ref. [36] it could be as strong as $M_0 \simeq 28$ keV (95% CL). Let us start by considering the most conservative bound $M_0 = 10$ keV.[7]

The dependence of $\langle q \rangle_s / \langle q \rangle_a$ on M_1 and the lepton asymmetry is shown in Fig. 6. Quite interestingly, this ratio can decrease to 0.3 (or 0.4 at small M_1, cf. end of Sec. 4) for a certain range of asymmetries. However, $\langle q \rangle_s / \langle q \rangle_a$ does not decrease further with increasing asymmetry, but increases again. Therefore, the lower limit $M_0 = 10$ keV corresponds to $M_1 \gtrsim 4$ keV.

Combining now the two constraints (from X-rays, Fig. 4, and from structure formation, Eq. (5.1)), we observe that a solution satisfying both constraints exists for $n_{\nu_e}/s \gtrsim 8 \times 10^{-6}$. The solution corresponds to masses $M_1 \simeq 4 - 25$ keV and mixing angles $\sin^2 2\theta \simeq 8 \times 10^{-10} - 2 \times 10^{-12}$. If the lepton asymmetry is increased, larger masses and smaller mixing angles become possible.

Let us then consider the case $M_0 \simeq 28$ keV [36]. Using the minimal value $\langle q \rangle_s / \langle q \rangle_a \sim 0.3$, $M_0 \simeq 28$ keV corresponds to $M_1 \gtrsim 28 \times 0.3 \simeq 8.4$ keV according to Eq. (5.1). Combining this with the X-ray constraints in Fig. 4, we see that this can in fact be satisfied with the same asymmetry as before, $n_{\nu_e}/s \gtrsim 8 \times 10^{-6}$.

It should be stressed, however, that the validity of Eq. (5.1) for spectra as extreme as those in Fig. 5 remains to be cross-checked. Nevertheless, if true, we can establish the absolute lower bound $M_1 \geq 4$ keV for sterile neutrinos capable of accounting for all of the dark matter in the Universe (assuming that the only mechanism for dark matter sterile neutrino production is active-sterile mixing).

6. Conclusions

The νMSM, i.e. Minimal Standard Model extended by three right-handed neutrinos with masses smaller than the electroweak scale, has a number of parameters not appearing in the Standard Model: three Majorana masses and a 3×3 complex matrix of Yukawa couplings. In ref. [1], the part of the parameter space associated with the two heaviest right-handed neutrinos was explored in detail, and a phenomenologically interesting corner was identified. Specifically, it was found that if the mass difference of the heavy (dominantly right-handed) neutrino mass eigenstates is much *smaller* than the known mass differences of the light (dominantly left-handed) mass eigenstates (**Scenario IIa**), then it is possible to explain the known active neutrino mass differences and mixings, and simultaneously generate and subsequently maintain a significant lepton asymmetry in the Universe, without violating constraints related to Big Bang Nucleosynthesis at temperatures of about 0.1 MeV.

[7] In this work we only consider lower bounds on the mass of the dark matter particle from structure formation. However, the problems of missing satellites and cuspy profiles in Cold Dark Matter cosmological models, as well as that of the galactic angular momentum, suggest that an upper bound may exist as well [55].

The purpose of the present paper has been to constrain the parameters associated with the lightest of the right-handed neutrinos, referred to with the subscript "1". In this case there are no constraints from the known active neutrino mass differences and mixings; rather, the contribution from the lightest right-handed neutrinos to the see-saw formulae is much below 0.01 eV. (Consequently the νMSM excludes the case of degenerate active neutrinos with a common mass scale $\gg 0.01$ eV; in particular, the effective mass for neutrinoless double beta decay cannot exceed 0.05 eV [56].) In contrast, the assertion that all of dark matter be made of these neutrinos does allow us to place further constraints on the parameters. More precisely, we were led in Sec. 5 to the mass range $M_1 \simeq 4 \ldots 50$ keV. The lower bound originates from combining the theoretical analysis of the present paper with observational X-ray (Fig. 4) and structure formation (Eq. (5.1), Fig. 6) constraints, whereas the upper bound is dictated by the maximal lepton asymmetry allowed by Big Bang Nucleosynthesis. The absolute values of the Yukawa couplings of the lightest right-handed neutrinos should be in the range $5 \times 10^{-15} \ldots 4 \times 10^{-13}$ in this case.

Of course, these constraints are relaxed if the sterile neutrinos only account for a fraction of the dark matter (see, e.g., ref. [57]); if a part of them are produced by some non-equilibrium mechanism not related to active-sterile mixing (see, e.g., refs. [37, 38, 39]); or if the thermal history of the Universe is non-standard (see, e.g., refs. [40, 41, 42]).

It is important to stress, in addition, that the lower bound $M_1 \gtrsim 4$ keV relies on a naive re-interpretation of structure formation simulations which were carried out assuming a thermal spectrum of dark matter particles, rather than a proper non-equilibrium shape as given in Fig. 5. Hopefully this issue can be put on more solid ground soon.

Finally, we recall that perhaps the most realistic hope for an experimental detection of dark matter sterile neutrinos in the parameter range that we have discussed, would be through the discovery of a peak in the diffuse X-ray background from regions where dark matter decays. The dominant decay channel is $N_1 \to \nu\gamma$ and the spectrum should thus peak at the energy $M_1/2 \gtrsim 2$ keV. As far as laboratory searches are concerned, they are quite difficult due to the very small Yukawa couplings of the dark matter sterile neutrinos; however, a possibility has been suggested in ref. [58].

Acknowledgements

We thank Alexey Boyarsky and Oleg Ruchayskiy for providing the X-ray data plotted in Fig. 4 and for helpful remarks. The work of M.L. was supported in part by the National Science Foundation, under Grant No. PHY05-51164, and that of M.S. by the Swiss National Science Foundation. We thank Takehiko Asaka for collaboration at initial stages of this work.

Appendix A. Different characterizations of lepton asymmetry

Several different conventions are used in the literature for characterizing the presence of a non-zero lepton asymmetry, and for completeness we specify the relations between them here. In analogy with the characterization of the baryon asymmetry through n_B/s, the conceptually cleanest way is to give the ratio of lepton asymmetry density over the total entropy density, because this quantity remains constant as a function of the temperature (as long as the Universe remains in thermodynamic equilibrium). However there are many leptonic species, so we need to specify which ones to count; in this paper we have assumed that the asymmetries are equal in all active leptons (both left-handed and right-handed), and choose the electron-like neutrinos (two degrees of freedom, particles and antiparticles) as a representative. The corresponding asymmetry, "particles minus antiparticles", normalised to the entropy density, is then denoted by n_{ν_e}/s.

Another way to express the asymmetry is to give the leptonic chemical potential, μ_L, that corresponds to n_{ν_e}. This is useful, since chemical potential is the quantity that appears in quantum field theoretic computations. In the free limit,

$$n_{\nu_e} = \langle \hat{\bar{\nu}}_{eL} \gamma_0 \hat{\nu}_{eL} \rangle = 2i \sum\!\!\!\!\!\!\int_{Q_{\rm f}} \frac{\tilde{q}_0}{\tilde{Q}^2 + m^2} \bigg|_{\tilde{q}_0 = \omega_{\rm f} + i\mu_L} = \int \frac{{\rm d}^3\mathbf{q}}{(2\pi)^3} \Big[n_{\rm F}(E - \mu_L) - n_{\rm F}(E + \mu_L) \Big] \,, \quad \text{(A.1)}$$

where $Q_{\rm f}$ are the fermionic Matsubara momenta, $Q_{\rm f} \equiv (\omega_{\rm f}, \mathbf{q})$ with $\omega_{\rm f} \equiv 2\pi T(n + \frac{1}{2})$, $n \in \mathbb{Z}$; $\tilde{Q} \equiv (\tilde{q}_0, \mathbf{q}) \equiv Q_{\rm f} + (i\mu_L, \mathbf{0})$; and $E \equiv \sqrt{\mathbf{q}^2 + m^2}$. In the massless limit $m \ll T$, Eq. (A.1) evaluates to

$$n_{\nu_e} = \frac{\mu_L T^2}{6} + \frac{\mu_L^3}{6\pi^2} \,. \quad \text{(A.2)}$$

Therefore, for $\mu_L \ll T$,

$$\frac{n_{\nu_e}}{s} \approx \frac{15}{4\pi^2 h_{\rm eff}} \times \frac{\mu_L}{T} \,, \quad \text{(A.3)}$$

where $h_{\rm eff}$ parametrizes the total entropy density through $s \equiv 2\pi^2 T^3 h_{\rm eff}/45$.

Yet another way to characterize the asymmetry is to use the "intuitive" measure of the asymmetry that one is naturally lead to in Boltzmann-equation or density-matrix type treatments, where the basic degrees of freedom are on-shell particle states:

$$\Delta \equiv \frac{\#_{\nu_e} - \#_{\bar{\nu}_e}}{\#_{\nu_e} + \#_{\bar{\nu}_e}} = \frac{n_{\nu_e}}{n_{\rm eq}} \,, \quad \text{(A.4)}$$

where $n_{\rm eq} \equiv \#_{\nu_e} + \#_{\bar{\nu}_e} \equiv 2\int {\rm d}^3\mathbf{q}/(2\pi)^3/(e^{q/T} + 1) = 3\zeta(3)T^3/2\pi^2$. Then we get

$$\frac{n_{\nu_e}}{s} = \frac{135\zeta(3)}{4\pi^4 h_{\rm eff}} \times \Delta \,. \quad \text{(A.5)}$$

Or, one can normalize with respect to the photon density,

$$L \equiv \frac{n_{\nu_e}}{n_\gamma} \,, \quad \text{(A.6)}$$

where $n_\gamma \equiv 2\int \mathrm{d}^3\mathbf{q}/(2\pi)^3/(e^{q/T}-1) = 2\zeta(3)T^3/\pi^2$, which yields

$$\frac{n_{\nu_e}}{s} = \frac{45\zeta(3)}{\pi^4 h_{\rm eff}} \times L \; . \tag{A.7}$$

Numerically, choosing to cite the temperature-dependent asymmetries $(\mu_L/T, \Delta, L)$ at $T = 100$ GeV as e.g. in refs. [9, 51], we may approximate $h_{\rm eff} \approx 102$ for the MSM,[8] whereby

$$\frac{n_{\nu_e}}{s} \approx 3.7 \times 10^{-3} \times \left.\frac{\mu_L}{T}\right|_{T\,=\,100\ \mathrm{GeV}} \tag{A.8}$$

$$\approx 4.1 \times 10^{-3} \times \left.\Delta\right|_{T\,=\,100\ \mathrm{GeV}} \tag{A.9}$$

$$\approx 5.4 \times 10^{-3} \times \left. L\right|_{T\,=\,100\ \mathrm{GeV}} \; . \tag{A.10}$$

References

[1] M. Shaposhnikov, arXiv:0804.4542 [hep-ph].

[2] X. Shi and G.M. Fuller, Phys. Rev. Lett. 82 (1999) 2832 [astro-ph/9810076].

[3] T. Asaka, S. Blanchet and M. Shaposhnikov, Phys. Lett. B 631 (2005) 151 [hep-ph/0503065].

[4] T. Asaka and M. Shaposhnikov, Phys. Lett. B 620 (2005) 17 [hep-ph/0505013]; M. Shaposhnikov, Nucl. Phys. B 763 (2007) 49 [hep-ph/0605047].

[5] S. Dodelson and L.M. Widrow, Phys. Rev. Lett. 72 (1994) 17 [hep-ph/9303287].

[6] A.D. Dolgov and S.H. Hansen, Astropart. Phys. 16 (2002) 339 [hep-ph/0009083].

[7] K. Abazajian, G.M. Fuller and M. Patel, Phys. Rev. D 64 (2001) 023501 [astro-ph/0101524].

[8] K. Abazajian, G.M. Fuller and W.H. Tucker, Astrophys. J. 562 (2001) 593 [astro-ph/0106002].

[9] K.N. Abazajian and G.M. Fuller, Phys. Rev. D 66 (2002) 023526 [astro-ph/0204293].

[10] K. Abazajian, Phys. Rev. D 73 (2006) 063506 [astro-ph/0511630].

[11] T. Asaka, M. Laine and M. Shaposhnikov, JHEP 06 (2006) 053 [hep-ph/0605209].

[12] T. Asaka, M. Laine and M. Shaposhnikov, JHEP 01 (2007) 091 [hep-ph/0612182].

[13] W. Guo, Phys. Rev. D 77 (2008) 033005 [arXiv:0709.1632].

[8] Refs. [50, 12] give estimates for $h_{\rm eff}$ from this range down to low temperatures, $T \sim 1$ MeV, taking into account radiative corrections due to strong interactions.

[14] C.T. Kishimoto and G.M. Fuller, arXiv:0802.3377 [astro-ph].

[15] A. Kusenko and G. Segrè, Phys. Lett. B 396 (1997) 197 [hep-ph/9701311]; G.M. Fuller, A. Kusenko, I. Mocioiu and S. Pascoli, Phys. Rev. D 68 (2003) 103002 [astro-ph/0307267]; M. Barkovich, J.C. D'Olivo and R. Montemayor, Phys. Rev. D 70 (2004) 043005 [hep-ph/0402259]; M. Mapelli, A. Ferrara and E. Pierpaoli, Mon. Not. Roy. Astron. Soc. 369 (2006) 1719 [astro-ph/0603237]; E. Ripamonti, M. Mapelli and A. Ferrara, Mon. Not. Roy. Astron. Soc. 374 (2007) 1067 [astro-ph/0606482]; E. Ripamonti, M. Mapelli and A. Ferrara, Mon. Not. Roy. Astron. Soc. 375 (2007) 1399 [astro-ph/0606483]; P.L. Biermann and A. Kusenko, Phys. Rev. Lett. 96 (2006) 091301 [astro-ph/0601004]; J. Stasielak, P.L. Biermann and A. Kusenko, Astrophys. J. 654 (2007) 290 [astro-ph/0606435]; F. Munyaneza and P.L. Biermann, Astron. Astrophys. 458 (2006) L9 [astro-ph/0609388]; J. Hidaka and G.M. Fuller, Phys. Rev. D 74 (2006) 125015 [astro-ph/0609425]; M.C. Richter, G.B. Tupper and R.D. Viollier, JCAP 12 (2006) 015 [astro-ph/0611552]; K. Petraki, arXiv:0801.3470 [hep-ph]; A. Kusenko, B.P. Mandal and A. Mukherjee, arXiv:0801.4734 [astro-ph].

[16] E.K. Akhmedov, V.A. Rubakov and A.Y. Smirnov, Phys. Rev. Lett. 81 (1998) 1359 [hep-ph/9803255].

[17] F.L. Bezrukov and M. Shaposhnikov, Phys. Lett. B 659 (2008) 703 [arXiv:0710.3755].

[18] M. Shaposhnikov, arXiv:0708.3550 [hep-th].

[19] K.A. Meissner and H. Nicolai, Phys. Lett. B 648 (2007) 312 [hep-th/0612165].

[20] A. Boyarsky, A. Neronov, O. Ruchayskiy and M. Shaposhnikov, Mon. Not. Roy. Astron. Soc. 370 (2006) 213 [astro-ph/0512509].

[21] A. Boyarsky, A. Neronov, O. Ruchayskiy and M. Shaposhnikov, Phys. Rev. D 74 (2006) 103506 [astro-ph/0603368].

[22] A. Boyarsky, A. Neronov, O. Ruchayskiy, M. Shaposhnikov and I. Tkachev, Phys. Rev. Lett. 97 (2006) 261302 [astro-ph/0603660].

[23] S. Riemer-Sørensen, S.H. Hansen and K. Pedersen, Astrophys. J. 644 (2006) L33 [astro-ph/0603661].

[24] S. Riemer-Sørensen, K. Pedersen, S.H. Hansen and H. Dahle, Phys. Rev. D 76 (2007) 043524 [astro-ph/0610034].

[25] A. Boyarsky, J. Nevalainen and O. Ruchayskiy, Astron. Astrophys. 471 (2007) 51 [astro-ph/0610961].

[26] K.N. Abazajian, M. Markevitch, S.M. Koushiappas and R.C. Hickox, Phys. Rev. D 75 (2007) 063511 [astro-ph/0611144].

[27] A. Boyarsky, O. Ruchayskiy and M. Markevitch, Astrophys. J. 673 (2008) 752 [astro-ph/0611168].

[28] A. Boyarsky, J.W. den Herder, A. Neronov and O. Ruchayskiy, Astropart. Phys. 28 (2007) 303 [astro-ph/0612219].

[29] H. Yüksel, J.F. Beacom and C.R. Watson, arXiv:0706.4084 [astro-ph].

[30] A. Boyarsky, D. Iakubovskyi, O. Ruchayskiy and V. Savchenko, arXiv:0709.2301 [astro-ph].

[31] A. Boyarsky, D. Malyshev, A. Neronov and O. Ruchayskiy, arXiv:0710.4922 [astro-ph].

[32] S.H. Hansen, J. Lesgourgues, S. Pastor and J. Silk, Mon. Not. Roy. Astron. Soc. 333 (2002) 544 [astro-ph/0106108].

[33] M. Viel, J. Lesgourgues, M.G. Haehnelt, S. Matarrese and A. Riotto, Phys. Rev. D 71 (2005) 063534 [astro-ph/0501562].

[34] U. Seljak, A. Makarov, P. McDonald and H. Trac, Phys. Rev. Lett. 97 (2006) 191303 [astro-ph/0602430].

[35] M. Viel, J. Lesgourgues, M.G. Haehnelt, S. Matarrese and A. Riotto, Phys. Rev. Lett. 97 (2006) 071301 [astro-ph/0605706].

[36] M. Viel, G.D. Becker, J.S. Bolton, M.G. Haehnelt, M. Rauch and W.L.W. Sargent, Phys. Rev. Lett. 100 (2008) 041304 [arXiv:0709.0131].

[37] M. Shaposhnikov and I. Tkachev, Phys. Lett. B 639 (2006) 414 [hep-ph/0604236].

[38] A. Kusenko, Phys. Rev. Lett. 97 (2006) 241301 [hep-ph/0609081].

[39] K. Petraki and A. Kusenko, arXiv:0711.4646 [hep-ph].

[40] G. Gelmini, S. Palomares-Ruiz and S. Pascoli, Phys. Rev. Lett. 93 (2004) 081302 [astro-ph/0403323]; G. Gelmini, E. Osoba, S. Palomares-Ruiz and S. Pascoli, arXiv:0803.2735 [astro-ph].

[41] C.E. Yaguna, JHEP 06 (2007) 002 [arXiv:0706.0178].

[42] S. Khalil and O. Seto, arXiv:0804.0336 [hep-ph].

[43] K. Kohri, M. Kawasaki and K. Sato, Astrophys. J. 490 (1997) 72 [astro-ph/9612237].

[44] A.D. Dolgov, S.H. Hansen, S. Pastor, S.T. Petcov, G.G. Raffelt and D.V. Semikoz, Nucl. Phys. B 632 (2002) 363 [hep-ph/0201287].

[45] W.-M. Yao *et al.* [Particle Data Group], J. Phys. G 33 (2006) 1.

[46] E. Komatsu *et al.* [WMAP Collaboration], arXiv:0803.0547 [astro-ph].

[47] I. Affleck and M. Dine, Nucl. Phys. B 249 (1985) 361.

[48] D. Nötzold and G. Raffelt, Nucl. Phys. B 307 (1988) 924.

[49] D. Boyanovsky and C.M. Ho, Phys. Rev. D 76 (2007) 085011 [arXiv:0705.0703].

[50] M. Laine and Y. Schröder, Phys. Rev. D 73 (2006) 085009 [hep-ph/0603048].

[51] K. Abazajian and S.M. Koushiappas, Phys. Rev. D 74 (2006) 023527 [astro-ph/0605271].

[52] S. Tremaine and J.E. Gunn, Phys. Rev. Lett. 42 (1979) 407.

[53] D.N.C. Lin and S.M. Faber, Astrophys. J. 266 (1983) L21.

[54] J.J. Dalcanton and C.J. Hogan, Astrophys. J. 561 (2001) 35 [astro-ph/0004381]; C.J. Hogan and J.J. Dalcanton, Phys. Rev. D 62 (2000) 063511 [astro-ph/0002330].

[55] B. Moore *et al.*, Astrophys. J. 524 (1999) L19 [astro-ph/9907411]; P. Bode, J.P. Ostriker and N. Turok, Astrophys. J. 556 (2001) 93 [astro-ph/0010389]; T. Goerdt *et al.*, Mon. Not. Roy. Astron. Soc. 368 (2006) 1073 [astro-ph/0601404]; G. Gilmore *et al.*, astro-ph/0703308; J. Sommer-Larsen and A. Dolgov, Astrophys. J. 551 (2001) 608 [astro-ph/9912166]; D. Boyanovsky, H.J. de Vega and N. Sanchez, Phys. Rev. D 77 (2008) 043518 [arXiv:0710.5180].

[56] F.L. Bezrukov, Phys. Rev. D 72 (2005) 071303 [hep-ph/0505247].

[57] A. Palazzo, D. Cumberbatch, A. Slosar and J. Silk, Phys. Rev. D 76 (2007) 103511 [arXiv:0707.1495].

[58] F.L. Bezrukov and M. Shaposhnikov, Phys. Rev. D 75 (2007) 053005 [hep-ph/0611352].